JOURNAL
OF THE AMERICAN CHEMICAL SOCIETY

VOLUME 99, NUMBER 23 NOVEMBER 9, 1977

Monte Carlo Calculations in the Isothermal–Isobaric Ensemble. 1. Liquid Water[1]

John C. Owicki[2a] and Harold A. Scheraga*[2b]

Contribution from the Department of Chemistry, Cornell University, Ithaca, New York 14853. *Received February 10, 1977*

Abstract: A Monte Carlo simulation of liquid water is carried out in the isothermal-isobaric ensemble at 298 K and atmospheric pressure. Simple cubic and face-centered cubic periodic boundary conditions are used with 64 and 100 water molecules, respectively. A number of thermodynamic properties are calculated, including the mean molar volume. Since quantum effects on the thermodynamic properties of water are nontrivial, and since the Monte Carlo procedure is based on classical statistical mechanics, quantum corrections to the computed internal energy and heat capacity are calculated. Use is made of energy probability distribution functions as aids in understanding the hydrogen-bonding interactions in the liquid. It is found that there is a broad, smooth distribution of hydrogen-bond energy in this model for liquid water, rather than relatively discrete sets of bonded and unbonded interaction energies. The use of Monte Carlo techniques to calculate free energies is discussed briefly, and the inadequacy of one published method is demonstrated.

I. Introduction

The chemical and physical properties of liquid water have a profound influence on processes in disciplines as diverse as geophysics and biochemistry. Water also is important in statistical mechanics as one of the simplest fluids whose structure is determined largely by strong, noncentral attractive forces (hydrogen bonds) rather than primarily by short-range overlap repulsions. It is hardly surprising, then, that a great deal of research effort has been devoted to the subject; a bibliography[3] on water, covering 1969–1974, cited about 2000 publications by 2800 authors. Of the advances during this period, some of the most fundamental have resulted from the use of Monte Carlo (MC)[4-8] and molecular dynamics (MD)[9-13] computer calculations.

All previous MC and MD studies of water and aqueous solutions have been carried out at fixed volume, It often would be advantageous to carry out theoretical calculations at constant pressure, particularly to study volume effects and to model processes taking place at constant pressure.

We, therefore, have performed a series of MC calculations in the isothermal-isobaric ensemble, i.e., with fixed temperature, pressure, and number of molecules. This paper reports the findings obtained for pure water, and its companion paper[14] presents the results for dilute aqueous solutions of methane.

In the present paper, section II is a resumé of some of the most relevant results of statistical mechanics. Section III includes a sketch of the important approaches to the theory of liquids, as well as a comparison of MC and MD. Section IV describes the MC technique in more detail, and section V discusses the intermolecular pair potential energy function used in these calculations. Technical computational details are covered in section VI. Section VII is a presentation of the results of the calculations, with discussion and comparison with experiment. Section VIII is devoted to a discussion of a previously proposed method for the MC calculation of free energies. Finally, the findings are summarized and conclusions are drawn in section IX.

II. Statistical Mechanics

A. Introduction. This section is the classical statistical-mechanical groundwork for the rest of the paper. For further information, the reader should consult Ben-Naim's book[15] or a standard text on the theory of liquids[16] or on statistical mechanics.[17]

We consider a system of N water molecules at absolute temperature T (with $\beta = 1/kT$), volume V, and pressure P (not all of which are independent variables). Summations and products are taken over molecular indices, from 1 to N, unless otherwise indicated. Integrations over molecular coordinates are evaluated over all parts of configuration space with the molecules confined to the volume V.

B. Description of Molecules. In this paper, water molecules are treated as rigid bodies; in other words, there are no intramolecular degrees of freedom. The six external degrees of freedom are taken to be the Cartesian coordinates (x, y, z) of the oxygen nucleus (arbitrarily treated as the "center" of the molecule) and three Euler angles[15] (ϕ, θ, ψ) specifying the rotational position about the center. ϕ and θ are the spherical azimuthal and polar angles specifying the orientation of the molecular C_2 axis, and ψ specifies the rotational degree of freedom about that axis. The vector of coordinates of molecule i is $\mathbf{X}_i = (x_i, y_i, z_i, \phi_i, \theta_i, \psi_i)$, and the collective coordinates of the N molecules are denoted by $\mathbf{X}^N = (x_1, y_1, z_1, \phi_1, \theta_1, \psi_1, x_2, \ldots, \psi_N)$. Also, $d\mathbf{X}^N = dx_1dy_1dz_1d\phi_1d\theta_1d\psi_1dx_2 \ldots d\psi_N$.

The configurations of molecules can be represented in many coordinate systems, and integrals over configurations must be

corrected for any alteration of configuration space if the coordinate system is changed from a Cartesian to some other one. This is accomplished by including the appropriate Jacobian function J in the integrand.[15,18] In the present coordinate system,

$$J(\mathbf{X}^N) = \prod_i \sin\theta_i \tag{1}$$

The differential volume element in configuration space at the point $\mathbf{X}^N$ is $J(\mathbf{X}^N)\mathrm{d}\mathbf{X}^N$.

C. Intermolecular Potential Energy. The interaction potential among the N molecules is $U_N(\mathbf{X}^N)$. We make the usual approximation that U_N is the sum of pair potential terms U:

$$U_N = \sum_{i>j} U(\mathbf{X}_i, \mathbf{X}_j) \tag{2}$$

The exact functional form chosen for U will be presented in section V.

D. Partition Functions and Ensembles. In the canonical ensemble (fixed T, V, N), the partition function is

$$Q(T, V, N) = \frac{q^N}{(8\pi^2)^N \Lambda^{3N} N!} Z(T, V, N) \tag{3}$$

where q is the classical rigid-body rotational momentum partition function and Λ is the thermal de Broglie wavelength. Z is the configuration integral, defined as

$$Z(T, V, N) = \int \cdots \int_{V^N} \exp[-\beta U_N(\mathbf{X}^N)] J(\mathbf{X}^N)\mathrm{d}\mathbf{X}^N \tag{4}$$

The Helmholtz free energy A is given by

$$A(T, V, N) = -kT \ln [Q(T, V, N)] \tag{5}$$

and the probability density for observing the system in some configuration $\mathbf{X}^N$ is $\pi(\mathbf{X}^N)$, where

$$\pi(\mathbf{X}^N) = \exp[-\beta U_N(\mathbf{X}^N)] J(\mathbf{X}^N)/Z(T, V, N) \tag{6}$$

Calculations can be carried out at fixed pressure rather than at fixed volume. The statistical mechanical ensemble corresponding to these conditions is the isothermal–isobaric or (T, P, N) ensemble. Its partition function and the canonical partition function are related as transforms of the conjugate variables P and V:

$$\Delta(T, P, N) = c \int_0^\infty Q(T, V, N) \exp(-\beta PV)\mathrm{d}V = \frac{cq^N}{(8\pi^2)^N \Lambda^{3N} N!} Z(T, P, N) \tag{7}$$

where c is a factor with dimensions of inverse volume introduced because of the transformation,[19,20] and

$$Z(T, P, N) = \int_0^\infty Z(T, V, N) \exp(-\beta PV)\mathrm{d}V \tag{8}$$

The Gibbs free energy G is given by

$$G(T, P, N) = -kT \ln [\Delta(T, P, N)] \tag{9}$$

The (T, P, N) configurational probability density is defined to include the volume as a variable:

$$\pi(\mathbf{X}^N, V) = \exp[-\beta U_N(\mathbf{X}^N) - \beta PV] J(\mathbf{X}^N)/Z(T, P, N) \tag{10}$$

It can be seen from eq 10 that the factor multiplying $Z(T, P, N)$ in eq 7 does not appear in the expression for $\pi(\mathbf{X}^N, V)$. For the rest of this section, we shall use the (T, P, N) ensemble; most expressions derived below have analogues in the (T, V, N) ensemble.

E. Ensemble Averages. For a general function $F(\mathbf{X}^N, V)$ we define $\langle F \rangle$ to be the ensemble average of F:

$$\langle F \rangle = \int_0^\infty \int \cdots \int_{V^N} F(\mathbf{X}^N, V)\pi(\mathbf{X}^N, V)\mathrm{d}\mathbf{X}^N\mathrm{d}V \tag{11}$$

For example, $\langle U_N \rangle$ is the mean (i.e., thermodynamic) potential energy of the system and $\langle V \rangle$ is its mean volume. The internal energy E is the sum of the kinetic energy E_K and U_N; the enthalpy H is the sum of the internal energy and PV. Hence,

$$\begin{aligned} \langle E \rangle &= \langle E_K \rangle + \langle U_N \rangle \\ \langle H \rangle &= \langle E \rangle + P\langle V \rangle \end{aligned} \tag{12}$$

Fluctuations in enthalpy and volume lead to three important thermodynamic functions:

a. Heat capacity

$$C_p \equiv (\partial\langle H \rangle/\partial T)_{P,N}/N = (\langle H^2 \rangle - \langle H \rangle^2)/NkT^2 \tag{13}$$

b. Isothermal compressibility

$$\kappa \equiv -(\partial\langle V \rangle/\partial P)_{T,N}/\langle V \rangle = (\langle V^2 \rangle - \langle V \rangle^2)/kT\langle V \rangle \tag{14}$$

c. Coefficient of thermal expansion

$$\alpha \equiv (\partial\langle V \rangle/\partial T)_{P,N}/\langle V \rangle = (\langle VH \rangle - \langle V \rangle\langle H \rangle)/kT^2\langle V \rangle \tag{15}$$

For computational purposes, it is convenient to rewrite the differences in a and c by expressing H in terms of its three component terms of eq 12. The resulting equations simplify somewhat because of the lack of correlation between E_K and U_N or V. There are no terms involving E_K in the expression for α, and C_p can be broken up into kinetic and potential contributions, as indicated below:

$$\begin{aligned} C_p &= C_{p,K} + C_{p,POT} \\ &= (\langle E_K^2 \rangle - \langle E_K \rangle^2)/NkT^2 + [\langle (U_N + PV)^2 \rangle \\ &\quad - \langle U_N + PV \rangle^2]/NkT^2 \end{aligned} \tag{16}$$

F. Probability Distribution Functions. It is possible to define a probability distribution function (PDF) for any function $F(\mathbf{X}^N, V)$:

$$P_F(\nu) \equiv \langle \delta[F(\mathbf{X}^N, V) - \nu] \rangle \tag{17}$$

The Dirac δ function ensemble average is the probability density that a configuration will occur for which F has the value ν. It follows easily that

$$\int_{-\infty}^\infty P_F(\nu)\mathrm{d}\nu = 1 \tag{18}$$

and

$$\langle F \rangle = \int_{-\infty}^\infty \nu P_F(\nu)\mathrm{d}\nu \tag{19}$$

A useful PDF is that for B, the molecular binding energy.[15] For the ith molecule,

$$B_i(\mathbf{X}^N) = \sum_{j \neq i} U(\mathbf{X}_i, \mathbf{X}_j) \tag{20}$$

Since the molecules are indistinguishable, the PDF can be based either on a specific molecule or on an average over all molecules; i.e.,

$$P_B(\nu) \equiv \frac{1}{N} \sum_j P_{B_j}(\nu) \tag{21}$$

which can be taken to be the same as $P_{B_i}(\nu)$. Thus, P_B describes the distribution of interaction energies of individual molecules with their surroundings.

It is possible[15,21] to extend the above definition of PDF's to form multidimensional and conditional PDF's. We will not go into detail on this subject except to introduce verbally a conditional PDF which we will use later. In a simple liquid, molecules are termed nearest neighbors when their centers approach closer than R_{NN}, the position of the first minimum in the radial distribution function. Thus, pairs corresponding to the first peak in the radial distribution function are nearest neighbors. We define $P_{UNN}(\nu)$ to be the PDF for pair potential energies involving only nearest-neighbor molecules. In water, P_{UNN} is a probe of the distribution of pair interaction energies between molecules which are close enough together to form hydrogen bonds or otherwise to interact strongly.

A familiar function in the theory of liquids, which is related closely to PDF's, is the atom-atom radial distribution function $g_{\alpha\beta}(R)$. In a molecular fluid with atoms of type α and β at number densities ρ_α and ρ_β, the probability density that an α and β are at a given pair of points a distance R apart is $\rho_\alpha\rho_\beta g_{\alpha\beta}(R)$.[16]

The mean number of atom centers of type β within a distance R of one of type α is given by

$$N_{\alpha\beta}(R) \equiv \rho_\beta \int_0^R 4\pi R^2 g_{\alpha\beta}(R)\mathrm{d}R \qquad (22)$$

As an important special case, $N_{OO}(R_{NN})$ is the coordination number of water.

III. Basic Techniques in the Theory of Liquids

A. Alternative Approaches. For all except the most trivial cases (e.g., ideal gas), the partition function of a dense fluid is extremely difficult to evaluate. This has led to three fundamentally different ways of approaching the problem of the statistical mechanics of liquids. In the first, a simplified partition function is constructed to represent what is believed to be the salient features of the system. There are many examples of this type for water, such as the cluster theory of Nemethy and Scheraga.[22] These theories have led to useful insights, but they are only as realistic as the drastically simplifying assumptions on which they are based.

Second, one can take the path of the classical theory of liquids.[16] This assumes a knowledge of the pair potential, and usually proceeds with the development of numerically solvable approximate integral equations for observable quantities. Water has been beyond the reach of such techniques, but some recent developments show promise.[23,24]

The third approach, that of MD or MC, also presumes a knowledge of the potential energy function. Numerical techniques are applied to obtain information while sidestepping the evaluation of the partition function. The resulting calculations consume great amounts of computer time, typically hours on large, modern machines. The strength of the MD and MC techniques is that, subject to limitations discussed below, they produce essentially exact results for the potential used.

B. Comparison of MD and MC. MD is a computer simulation in which molecules are assigned initial coordinates and momenta which are allowed to evolve in time by numerical integration of the differential equations of motion. Time average mechanical properties (both equilibrium and transport) can be obtained if the simulated time is long with respect to the periods of large fluctuations in these quantities. Since the energy, volume, and number of particles (E, V, N) are fixed, MD operates in the microcanonical ensemble.

As it usually is applied to calculations on liquids, MC also can be viewed as a simulation. More precisely, though, it is a stochastic numerical integration technique for obtaining ensemble averages. MC has not been used to compute transport properties of liquids, because they are not easy to formulate as time-independent ensemble averages. In this respect, it is not as powerful as MD. However, the much greater flexibility of MC calculations allows the use of various ensembles and various averaging procedures in the computation of quantities which would be practically impossible to compute with MD.[25,26] This flexibility dictated our choice of the MC method.

IV. The Monte Carlo Method

A. Introduction. The title of this section is misleading in that there actually are many Monte Carlo methods,[27] which are applied to a whole range of problems from game theory to nuclear physics and statistical mechanics. Much of the applicability of MC stems from the fact that, as the complexity and number of degrees of freedom in a problem become large, stochastic techniques often become the most efficient means of solution. MC calculations on liquids derive from the technique introduced by Metropolis et al.[28] in 1953, and all further discussion of MC here will refer to that algorithm.

B. The Metropolis Method in the (T, V, N) Ensemble. This algorithm is a technique for generating a series or chain (technically, a Markov chain) of configurations $\{\mathbf{X}_m{}^N\}$, $m = 1, 2, \ldots, M$, such that, as $M \to \infty$, $\{\mathbf{X}_m{}^N\}$ is distributed according to the canonical probability distribution function π. It follows that, for any $F(\mathbf{X}^N)$,

$$\lim_{M\to\infty} \frac{1}{M} \sum_{m=1}^{M} F(\mathbf{X}_m{}^N) = \langle F \rangle \qquad (23)$$

In practice, M is finite but large enough so that the MC average (which we shall denote by $\overline{F}$) converges sufficiently close to $\langle F \rangle$. We now turn to the algorithm itself. For further information and proofs, the reader should consult ref 19, 27, and 29.

Assume that there are a finite number of discrete values of $\mathbf{X}^N$, termed states of the system.[30] It will be convenient to denote the states $\{\mathbf{S}_s\}$, $s = 1, 2, \ldots$. Further assume that we already have generated m configurations of the chain, which currently is in state i (i.e., $\mathbf{X}_m{}^N = \mathbf{S}_i$). To find the next configuration in the chain, first randomly generate some trial configuration (see below), say $\mathbf{S}_j$. If $\pi_j \geq \pi_i$, set $\mathbf{X}_{m+1}{}^N = \mathbf{S}_j$ [where $\pi_i \equiv \pi(\mathbf{S}_i)$]. If $\pi_j < \pi_i$, set $\mathbf{X}_{m+1}{}^N = \mathbf{S}_j$ with probability π_j/π_i, and let $\mathbf{X}_{m+1}{}^N = \mathbf{S}_i$ with probability $(1 - \pi_j/\pi_i)$. The choice when $\pi_j < \pi_i$ is made by generating a random number r uniformly on the interval (0, 1). If $r < \pi_j/\pi_i$, $\mathbf{X}_{m+1}{}^N = \mathbf{S}_j$; otherwise, $\mathbf{X}_{m+1}{}^N = \mathbf{S}_i$.

Since the configuration integral Z is unknown, so are all the values of π (see eq 10). However, Z cancels when the ratio π_j/π_i is formed:

$$\pi_j/\pi_i = \exp\{-\beta[U_N(\mathbf{S}_j) - U_N(\mathbf{S}_i)]\}[J(\mathbf{S}_j)/J(\mathbf{S}_i)] \qquad (24)$$

This simplifies further when J is a constant, as for the Cartesian coordinates of point particles.

Trial configurations may be generated in many ways.[31,32] Usually, something like the following prescription is used: (1) pick a molecule at random; (2) for each coordinate of that molecule, pick a small random displacement uniformly on some interval $(-\delta, \delta)$, where δ is a constant which may be different for each coordinate. The addition of this perturbation to the current configuration generates the trial configuration. The values of the maximum step sizes δ are adjusted to achieve ~50% acceptance of the trial steps, so as to promote rapid convergence of the chain.

The ultimate convergence of the MC average is independent of the starting configuration, which generally is some highly improbable state. Finite averages, though, give undue weight to these configurations. One, therefore, discards the first part of the chain, beginning the averaging only after the functions to be averaged have settled down to fluctuations about the mean.

C. Periodic Boundary Conditions. Computational economy dictates that one use the smallest number of molecules which

adequately reproduces the properties of the liquid being studied. Surface effects render this number unfeasibly large if the system is a cluster of N molecules confined to the volume V. However, if the cluster (the base cell) is surrounded by replicas of itself on some periodic lattice, surface effects are reduced dramatically, and representative calculations are possible with $N \sim 10^1$ to 10^3, depending on the liquid being studied. These are the periodic boundary conditions (PBC) introduced by Metropolis et al.[28]

The usual lattice is simple cubic, so that the cells are also cubic. When the center of a perturbed molecule leaves the cell, the molecule is translated on the lattice so that it reenters the cell from the opposite face. The only pair potential interactions which are calculated are those for which at least one of the molecules is in the base cell.

The effects of the artificial correlations imposed by the PBC can be reduced if interactions beyond some cutoff distance R_c are not calculated. This also decreases the computation time. A correction may be made for these neglected interactions (see section VI). The "minimum-image" convention is often used, in which R_c is chosen so that a molecule i interacts with at most one image (the closest) of molecule j on the lattice[19] (or with molecule j itself if it is closer to i than any of its images are). By this criterion, R_c is one-half the distance separating any molecule from its closest image, and is a property of the lattice.

For the simple cubic lattice with cell side length $L = V^{1/3}$, this gives $R_c = L/2$. Of all lattices, a closest packing lattice such as face-centered cubic (FCC) produces the largest image separation, with a minimum-image convention value of $R_c = V^{1/3}/2^{5/6}$. The cells are rhombic dodecahedra, four of which occur in the overall cubic cell with lattice parameter $L = (4V)^{1/3}$. Under conditions where PBC correlations are a problem, it might be wise to use this lattice.

D. The Metropolis Method in the (T, P, N) Ensemble. This differs from the (T, V, N) ensemble method by the inclusion of the cell volume as a variable, to be perturbed randomly in the same way as the molecular coordinates. The definition of a state is expanded to include V, as well as the configuration. As described by Wood,[19] it is efficient to scale the Cartesian coordinates of the molecular centers by L and to work with fractional cell coordinates. This adds a factor of L^{3N} to the Jacobian. In the (T, P, N) ensemble, π_j/π_i also gains a PV term:

$$\pi_j/\pi_i = \exp\{-\beta[U_N(\mathbf{S}_j) - U_N(\mathbf{S}_i)] - \beta P(V_j - V_i)\}[J(\mathbf{S}_j)/J(\mathbf{S}_i)] \quad (25)$$

A volume change is not made in every step but only after some set number of steps involving the perturbation of only the molecular coordinates. The frequency of V steps is determined empirically: if it is too high, the computation time will be wasted;[33] if it is too low, the convergence of properties related to V will be poor.

A disadvantage of the (T, P, N) technique is that it requires more computer time to achieve a given level of precision than does the standard (T, V, N) method. This is due primarily to the added computational expense of perturbing the volume in the (T, P, N) ensemble.[33]

E. Error Analysis. Statistical tests[34] can be performed to estimate the standard errors of the computed MC averages. This involves a calculation of the ensemble averages over segments of the chain of configurations, and then an analysis of the fluctuations of these subaverages. Because of the high correlations between successive steps in the chain, there is a tendency to underestimate the error, and care must be exercised to ensure the validity of the error analysis.

V. Water-Water Pair Potential

A. Introduction. Over the past 10 years, several fairly realistic analytical empirical pair potentials have been developed for water.[35,36] Since the EPEN potential was not fully developed[36] at the time that this work was carried out, we used the CI potential of Matsuoka et al.,[37] which is the most successful to date in reproducing the structure and thermodynamics of liquid water.[8]

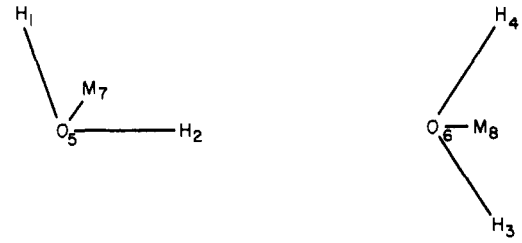

Figure 1. Numbering of points for CI potenital. The M point lies on the molecular C_2 axis.

Table I. Parameters for CI Water Pair Potential[a]

q^2 = 170.8842 kcal Å/mol	b_2 = 2.760870 Å^{-1}
a_1 = 1.088931 × 10^6 kcal/mol	b_3 = 2.961927 Å^{-1}
a_2 = 6.667210 × 10^2 kcal/mol	b_4 = 2.233281 Å^{-1}
a_3 = 1.455685 × 10^3 kcal/mol	R_{OM} = 0.2676451 Å
a_4 = 2.736156 × 10^2 kcal/mol	R_{OH} = 0.9572 Å
b_1 = 5.152759 Å^{-1}	∠H-O-H = 104.52°

[a] Parameters were taken from ref 37. R_{OH} and ∠H-O-H are the experimental geometry, as determined by Benedict et al.[38]

B. The CI Potential. Masuoka et al.[37] performed ab initio plus configuration-interaction (CI) calculations on a set of 66 water dimer configurations to obtain intermolecular potential energies. An analytical functional form was chosen, and its parameters were adjusted to obtain the best least-squares fit to the quantum-mechanical energies. The resulting CI potential is presented in eq 26 with points numbered as in Figure 1 and with the parameters[37,38] in Table I. The important features are the Coulombic interactions among hydrogen nuclei and "M" points, as well as exponential attractions and repulsions involving oxygen and hydrogen nuclei.

$$\begin{aligned} U = {} & q^2(1/R_{13} + 1/R_{14} + 1/R_{23} + 1/R_{24} + 4/R_{78} - 2/R_{18} \\ & - 2/R_{28} - 2/R_{37} - 2/R_{47}) + a_1 \exp(-b_1 R_{56}) \\ & + a_2[\exp(-b_2 R_{13}) + \exp(-b_2 R_{14}) + \exp(-b_2 R_{23}) \\ & + \exp(-b_2 R_{24})] \\ & + a_3[\exp(-b_3 R_{16}) + \exp(-b_3 R_{26}) + \exp(-b_3 R_{35}) \\ & + \exp(-b_3 R_{45})] \\ & - a_4[\exp(-b_4 R_{16}) + \exp(-b_4 R_{26}) + \exp(-b_4 R_{35}) \\ & + \exp(-b_4 R_{45})] \end{aligned} \quad (26)$$

where the subscripts on the R's indicate the pairs of atoms involved. This is a true pair potential, not an effective one; i.e., it does not have three- and higher body energy terms included in an average way.

C. Long Range Potential. When two water molecules are close (i.e., with the oxygen-oxygen distance $R_{OO} \sim 3$ Å), the potential energy surface is a complicated function of the configuration. Thus, an empirical potential energy function must also be complex to fit it well. Indeed, the CI potential has ten adjustable parameters and 22 additive terms. However, for larger separations, the molecules do not interact as strongly, and the potential energy surface simplifies. Since most computer time in MC and MD calculations is spent evaluating energies, and since most molecules are not adjacent, it is economically sensible to use a simplified long-range (LR) potential at large distances.

A good LR potential should satisfy three criteria. First, it should be computationally simpler than the fill potential.

Table II. Parameters for MC Calculations

Chain	T, K	P, atm	N	PBC	No. of steps × 10^{-5} Discarded	Averaged
I	298	1	64	Simple cubic	7.5	9.6
II	298	1	100	FCC	9.5	4.8

Chain	No. of $\mathbf{X}^N$ steps/ no. of V steps	Maximum coordinate step sizes $x/L, y/L, z/L$	ϕ, ψ, deg	Cos θ	V, Å^3
I	200	0.012	5	0.073	64
II	300	0.006	6	0.088	70

Second, it should be accurate. Third, discontinuities at the junction between the full and LR potentials should be small enough not to affect the properties of the system significantly. These are somewhat conflicting requirements.

After testing a variety of forms, we selected a three-parameter function with Lennard-Jones interaction between "M" points and Coulombic interactions among "M" points and hydrogen nuclei (as in the full CI potential):

$$U_{LR} = q_{LR}^2(1/R_{13} + 1/R_{14} + 1/R_{23} + 1/R_{24} + 4/R_{78} - 2/R_{18} - 2/R_{28} - 2/R_{37} - 2/R_{47}) - c/R_{78}^6 + d/R_{78}^{12} \quad (27)$$

On an IBM 370/168 computer, this executes about three times as fast as the CI potential.

Parametrization was carried out by a least-squares fit to the energies of two sets of configurations, selected as follows. Assume that the LR potential is to be used whenever $R_{OO} > R_J$, where R_J is the junction O-O distance. The first set of configurations was all the ab initio points used in the parametrization of the CI potential for which $R_{OO} > R_J$. The second set was a grid of configurations with $R_{OO} = R_J$, the energy being evaluated with eq 26. $R_J = 4.5$ Å seemed the best compromise between economy and accuracy; parametrization was carried out with 18 ab initio and 72 grid data points, with the two sets weighted equally in the least-squares algorithm. The resultant parameters were $q_{LR}^2 = 173.561$ kcal Å/mol, $c = 97.4680$ kcal Å^6/mol, and $d = 5.49168 \times 10^5$ kcal Å^{12}/mol. The fits were good. The root mean square deviation from the ab initio points was 0.059 kcal/mol, slightly better than the fit of the CI potential for the same points. For a set of 10 000 randomly selected dimer configurations with $R_{OO} = R_J$, the mean LR energy was 0.001 kcal/mol lower than the mean energy with the CI potential; the root mean square difference was 0.050 kcal/mol.

For still larger separations, $R_{OO} \gtrsim 6$-7 Å, it should be possible to parametrize a good dipole-dipole interaction potential, which would be still simpler. In this study, however, we did not calculate energies in that range (see section VI).[39]

VI. Computational Details

A. General. The computer program written for these calculations was checked[26] by successfully reproducing the results of MC calculations carried out on a Lennard-Jones fluid by McDonald and Singer.[40] For the computations on water, two chains were generated, both in the (T, P, N) ensemble. The major differences between the two were that 64 molecules and simple cubic PBC were used for chain I, while chain II had N = 100 with FCC PBC. The most important parameters are summarized in Table II. The initial configurations were constructed by assigning random positions and orientations to the molecules in the base cell, subject to the condition that molecular centers be separated by at least 2.6 Å.

B. Perturbation of θ. It should be recalled from sections IIB and IVD that the use of θ as a molecular coordinate requires the computation of ratios of Jacobians such as $\sin(\theta + \delta\theta)/\sin\theta$ in determining step acceptance probabilities. If $\cos\theta$ is substituted for θ as the coordinate to be perturbed, however, the dependence of the Jacobian on θ vanishes.[41] Thus, the Jacobians cancel in eq 24. This simplification (which we used in all computations) follows from the fact that $\sin\theta\, d\theta = -d(\cos\theta)$.

C. Interaction Cutoff Distance R_c. Interactions were not calculated between molecules whose centers were farther apart than $R_c = 6.35$ Å. This cutoff distance was chosen, on the basis of preliminary MC calculations, to be slightly smaller than the smallest minimum-image value of R_c which would be encountered during the volume fluctuations in chain I. It would have been possible to increase R_c for chain II, but, to save computer time, we did not. This should not vitiate the increased accuracy of the larger ensemble; we have corrected for the neglected interactions (see below), and the principal advantage of a larger value of N remains in the smaller artificial correlations imposed on the molecules by the PBC.

D. Corrections for Neglected Interactions. For $R_{OO} > R_c$, dispersion and dipole-dipole interactions are the largest terms in the pair potential. If the dispersion interaction is of the form $-C/R_{OO}^6$, and if there are no O-O correlations beyond R_c, then it is easy to show[42] that the statistical dispersion correction to U_N is

$$U_{disp} = -2\pi CN^2/(3VR_c^3) \quad (28)$$

The Kirkwood-Müller formula[43] can be used to estimate C = 1366 kcal Å^6/mol. U_{disp} was added to U_N for each configuration, and it averaged $\sim -0.3N$ kcal/mol for both chains.

The dipole-dipole correlations beyond R_c are difficult to treat adequately, but they are a small effect. We chose to include this correction as a perturbation on $\overline{U}_N$ at the end of the calculation, using the Onsager reaction field.[5] After every 10 000 steps in the chain, the configuration was stored for later analysis. The net dipole moment $\mathbf{M}$ in a sphere of radius R_c surrounding each molecule in each stored configuration was computed, and the dot product was taken with $\boldsymbol{\mu}$, the dipole moment of the central molecule. The dipole-dipole correction to $\overline{U}_N$ then was calculated as

$$\overline{U}_{\mu\mu} = -N(\epsilon - 1)\boldsymbol{\mu}\cdot\mathbf{M}/[(2\epsilon + 1)R_c^3] \quad (29)$$

ϵ is the experimental[44] dielectric constant, 78.5; μ was taken to be 2.19 D, as given by the CI potential charge distribution. Technically, $\overline{U}_{\mu\mu}$ is a free energy, but it is numerically almost identical with the internal energy of the reaction field. The values obtained for $\overline{U}_{\mu\mu}$ were $+0.15N$ kcal/mol for chain I and $+0.12N$ kcal/mol for chain II. These are of the same sign and magnitude as the results of the study by Watts under similar conditions.[5]

VII. Results and Discussion

A. Introduction. The principal thermodynamic quantities (and error estimates) computed in this study are collected in

Table III. Principal Thermodynamic Properties[a]

Property	Units	Exptl value	MC calcd value		
			Chain I[b]	Chain II[b]	(T, V, N)[c]
$\langle U_N \rangle / N$	kcal/mol		-9.38 ± 0.07	-9.07 ± 0.13	-8.51
$\langle E \rangle / N$	kcal/mol	-8.14[d]	-7.4 ± 0.3[e]	-7.1 ± 0.3[e]	-6.5 (± 0.3?)[e]
$C_{p,\mathrm{POT}}$	cal/mol deg		11 ± 2	17 ± 7	9.9[f]
C_p	cal/mol deg	18.0[g]	14.6 ± 2[h]	20.6 ± 7[h]	13.5 (± 2?)[f,h]
$\langle V \rangle / N$	cm^3/mol	18.07[g]	23.78 ± 0.07	23.81 ± 0.16	(18.07)[i]
κ	10^{-6}/atm	41[g]	38 ± 5	47 ± 16	53
α	10^{-5}/deg	27[j]	66 ± 10	39 ± 13	

[a] All quantities refer to $T = 298$ K, $P = 1$ atm. The experimental values, $\langle E \rangle$ and $\langle V \rangle$, correspond to $\overline{E}$ and $\overline{V}$ of the Monte Carlo calculation. [b] (T, P, N) ensemble; for chain I, $N = 64$; for chain II, $N = 100$. [c] Reference 8; $N = 343$; no error estimates were given. [d] Reference 45. [e] Calculated using estimates of the kinetic energy and quantum corrections discussed in Appendix. Indicated errors arise chiefly from uncertainties in these factors. [f] This is the constant-volume heat capacity, which experimentally is 0.2 cal/mol deg less than the isobaric quantity ($C_v = C_p - TV\alpha^2/\kappa$). [g] Reference 46. [h] Calculated using estimate of vibrational heat capacity as discussed in Appendix. [i] Volume fixed at experimental value. [j] Reference 47.

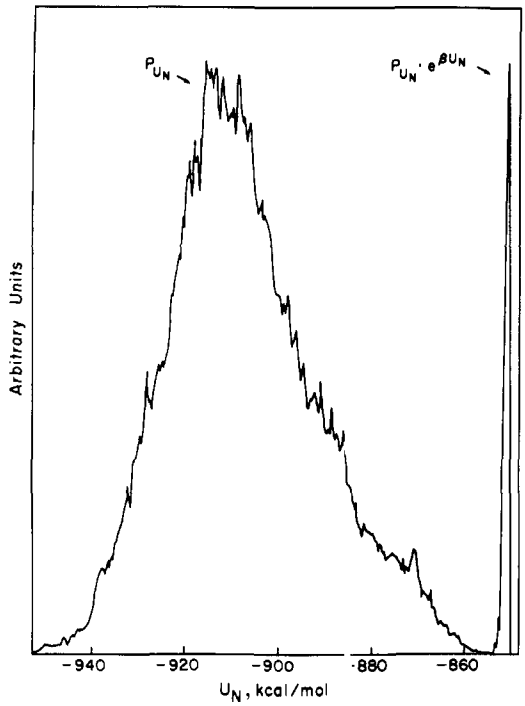

Figure 2. P_{U_N}, probability distribution function for U_n, as obtained for chain II. Spike at right is product $P_{U_N} \exp(\beta U_N)$, as discussed in section VIII. The ordinates for the two plots are different.

Table III. The results for chain II are generally more accurate than those for chain I, because of the larger value of N in chain II. The results for chain II are less precise (reproducible) than those for chain I, however, since they have a slightly higher statistical uncertainty than do those of chain I. Experimental values[45-47] are included in Table III for comparison, as are the MC results obtained by Lie, Clementi, and Yoshimine (henceforth LCY).[8] The LCY study was performed in the (T, V, N) ensemble with the same CI potential used here and at the same temperature; V was fixed at the experimental low-pressure value (for $P = 1$ atm), and 343 molecules were used.

The various distribution functions calculated in this study (Figures 2-7) have not been smoothed for presentation. This makes it easy to see the amount of statistical scatter in the data. Statistical uncertainties (see section IVE) are reported as "± 1 standard deviation."

B. Energy and Heat Capacity. The calculated (T, P, N) internal energies are somewhat too high. As LCY noted, the inclusion of three-body energetic effects would improve the agreement substantially. The effect of increasing N is to increase $\overline{U}_N/N$. This also was observed in the two (T, V, N) MC studies in which N was varied.[5,7] Together with the radial distribution function data discussed below, these facts suggest the generalization that the principal error introduced by using too few water molecules is to structure the liquid too highly.

The value of $\overline{U}_N/N$ of chain II is about 0.6 (± 0.2) kcal/mol below the LCY value obtained for the same experimental conditions. This difference can be traced to three factors. (1) Compared to LCY, we used a fairly small value of R_c; we treated nonelectrostatic interactions beyond this cutoff distance as dispersions, which were both stronger and longer ranged than the corresponding weak exponential terms in the CI potential. This contributes up to 0.3 kcal/mol to the energy difference. (2) The mean density in our calculations is lower than the experimental value, which tends to lower $\overline{U}_N$. (3) The dependence of $\overline{U}_N$ on N indicates that, if we had used $N > 100$, $\overline{U}_N$ would have increased slightly.

The calculated heat capacities are in fair agreement with those from experiment and LCY, when allowance is made for the large uncertainties in the calculated values. The relative standard errors in fluctuation quantities are expected to be larger than those in the parent averages,

The PDP for U_N, as computed in chain II, is presented in Figure 2. P_{U_N} is a fundamental function; its mean is $\overline{U}_N$, and its variance [i.e., $\overline{U_N^2} - (\overline{U}_N)^2$] is directly related to the heat capacity. There are no known experimental techniques for obtaining P_{U_N}.

C. Volume, Compressibility, Expansibility. The most significant disagreement between our calculations and experiment is the error in the average volume, corresponding to a 24% underestimate of the density. The observed dependence of $\overline{V}/N$ on N is negligible. In the LCY study, the analogue of the volume error was the poor value of the computed pressure.

Extensive calculations of the P-V-T behavior of water can be a sensitive test of a potential energy function. This sensitivity is exhibited in the fact that preliminary (T, P, N) MC calculations[48] show a significant improvement in the average volume using a pair potential with the improved EPEN functional form[36] but parametrized to the same ab initio data set used for the CI potential.

The experimental value of κ falls within the error limits of the computed (T, P, N) values, while the calculated values of α are too high. This is not surprising since α is a strong function of T, and thus should be hard to fit accurately.

D. Radial Distribution Functions. The calculated O-O, O-H, and H-H radial distribution functions are given in Figures 3-5, together with the experimental and LCY results. The experimental g_{OO} curve was obtained by x-ray diffraction;[49] the experimental g_{OH} and g_{HH} curves were obtained[50] by combining the x-ray data with neutron diffraction results on D_2O and a model for the short-range order in the liquid. It

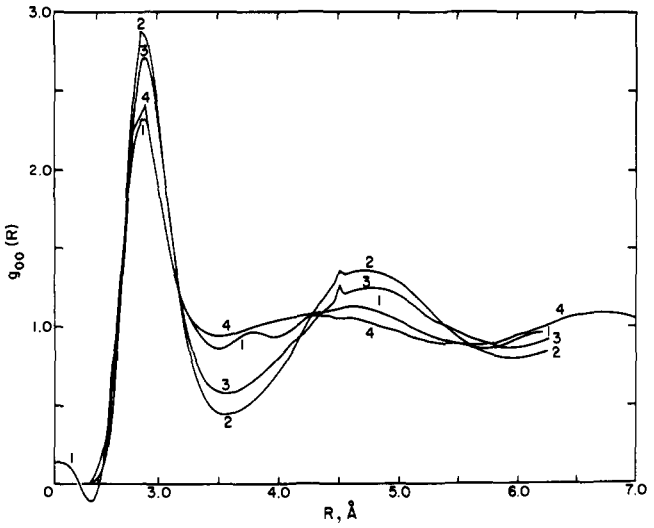

Figure 3. $g_{OO}(R)$, oxygen-oxygen radial distribution function. Legend: 1, experimental;[49] 2, calculated, chain I ($N = 64$); 3, calculated, chain II ($N = 100$); 4, calculated, (T, V, N) ensemble.[8]

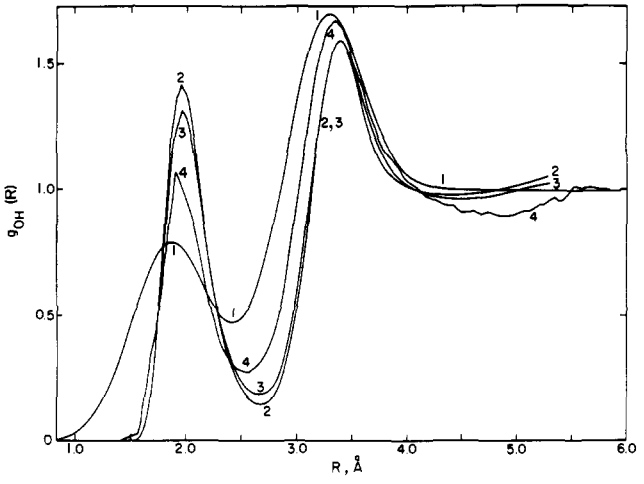

Figure 4. $g_{OH}(R)$, oxygen-hydrogen radial distribution function. Numbering of curves as in Figure 3.

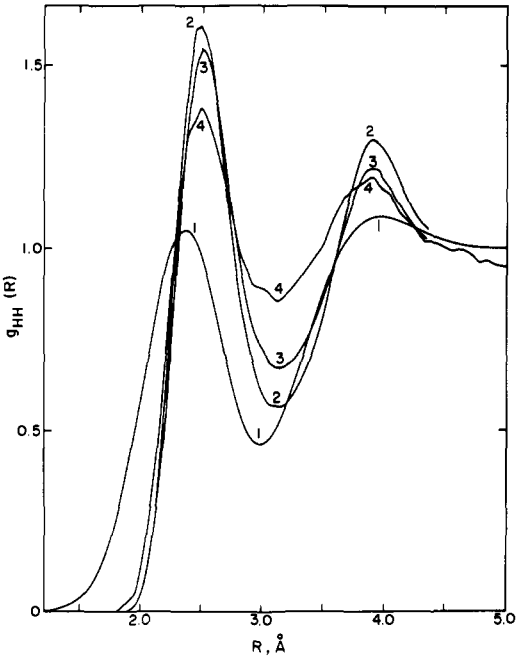

Figure 5. $g_{HH}(R)$, hydrogen-hydrogen radial distribution function. Numbering of curves as in Figure 3.

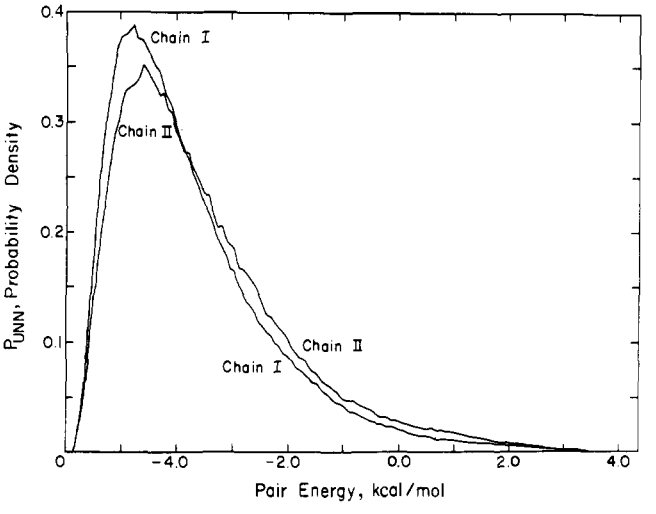

Figure 6. P_{UNN}, probability distribution function of nearest-neighbor pair potential interactions.

is likely that the experimental g_{OH} and g_{HH} curves are much less accurate than the g_{OO} curve.[7,8]

The (T, P, N) MC results reproduce the important features of the atom-atom correlations found experimentally and by LCY in the (T, V, N) ensemble.[51] The main difference is that the local (tetrahedral) order in the (T, P, N) functions tends to be sharper than in the other cases. This is related to the abnormally low average density and also the somewhat small value of N used. A comparison of the data for chains I and II indicates that, as N increases, the radial distribution functions level out somewhat.

The coordination number in water under these conditions (see eq 22) is ~5.2, both experimentally[49] and in the LCY study. For chains I and II, the results are 4.01 ± 0.02 and 4.05 ± 0.03, respectively, reflecting the lowered density. Although these values are only slightly higher than in ice (4.0), the radial distribution functions show that the system is fluid rather than crystalline. Also, energy and volume fluctuations characteristic of liquid-solid phase transitions in MC calculations did not occur during the generation of the MC chains.

E. Energy Distributions and Hydrogen Bonding. We now consider the question, "What is the nature of hydrogen bonding in liquid water?" While the general features are clear, there continues to be much debate about several important aspects of the question. One of these is whether it makes sense to speak of discrete "made" and "broken" hydrogen bonds, or whether instead there is a broad range of interaction energies varying continuously from strong to very weak. Another unresolved problem is whether the range of energetic environments of individual molecules is made up of two (or more) fairly discrete populations of molecules, or whether the distribution is more or less simple and continuous. By studying the two PDF's, P_{UNN} and P_B, introduced in section II, we have answered these questions for the present model of liquid water.

P_{UNN} is the distribution of pair potential interactions between molecules which are close enough together ($R_{NN} < 3.6$ Å) to be hydrogen bonded[52] if their orientations are energetically favorable. If the environment in the liquid segregates these pair interactions into "hydrogen-bonded" and "non-hydrogen-bonded" groups, P_{UNN} should have two peaks representing the two classes. This behavior is not observed in our calculations, which are displayed in Figure 6. P_{UNN} is a smooth, skewed, broad distribution with a single peak near −4.65 kcal/mol and a mean of −3.52 ± 0.07 kcal/mol for

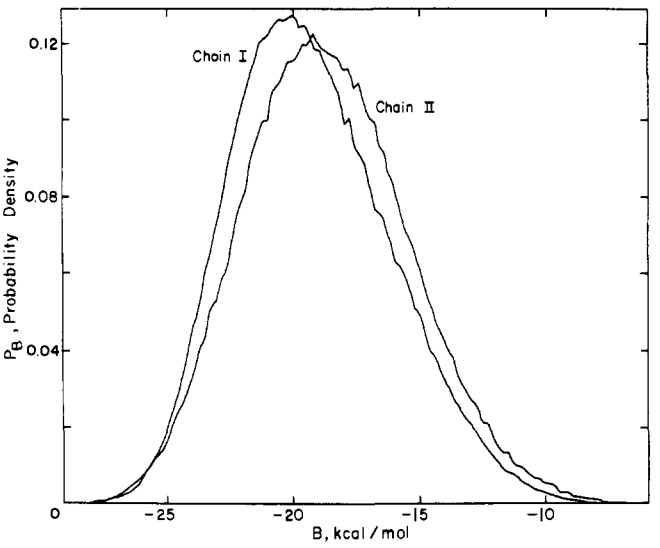

Figure 7. P_B, probability distribution function of binding energies B. The mean binding energy is twice the mean potential energy per molecule.

chain II, and at -4.80 and -3.74 ± 0.03 kcal/mol, respectively, for chain I. The shape of the distribution is fairly easy to understand. The probability density dies off at low energies because the volume of dimer configuration space with these energies is small, vanishing below the global pair energy minimum (~ -5.8 kcal/mol). There are many high-energy configurations, but P_{UNN} dies off in this region because of the unfavorable energetics. The peak in the middle is a compromise between these two factors. As an aside, we note that, since $P_{UNN} \sim 0$ for energies $\gtrsim 3$ kcal/mol, the properties of the liquid are almost completely insensitive to the behavior of the pair potential at energies above this value.[48]

Our analysis of P_B was motivated by the following suggestion by Ben-Naim.[15] For a simple liquid, P_B is unimodal, reflecting a simple distribution of energetic environments. In a MC study of a two-dimensional waterlike liquid with molecules capable of participating in up to three "hydrogen bonds," Ben-Naim found that the behavior of P_B was more complex. For suitable potential parameters, he observed a series of four maxima, corresponding in energies to molecules with from zero to three hydrogen bonds. It is natural to identify the peaks with four quasi-components in a generalized mixture model of the liquid; perhaps the situation in water might be analogous.[15]

However, the distribution of B computed in the present study (P_B, Figure 7) is unimodal and featureless; there is no evidence for shoulders on the peak. This result is consistent with our finding regarding the simple distribution of nearest-neighbor energies, since about 80% of the mean binding energy $\overline{B}$ is due to nearest-neighbor interactions.

The ascription of these structural features of the model liquid to water itself must be tempered by a recognition of the approximations in the simulation. Specifically, the structure may be influenced by the low calculated density.

VIII. Monte Carlo Calculation of Free Energies

A. Introduction. The calculation of free energies is an important problem in liquid theory. However, the Metropolis MC technique is poorly suited for carrying out such computations; the free energy is essentially the logarithm of the partition function, and the Metropolis algorithm is successful largely because it avoids the necessity of calculating the configuration integral, which is the most complicated part of this partition function (see section IVB and eq 24 and 25).

Nevertheless, it is possible[53] to write an expression for the free energy as an ensemble average which, in principle, can be evaluated by the usual Metropolis procedure. From eq 10 and 11,

$$\langle \exp(+\beta U_N) \rangle = \frac{1}{Z} \int_0^\infty \int \cdots \int_{V^N} \int [\exp(-\beta PV)] J(\mathbf{X}^N) d\mathbf{X}^N dV \quad (30)$$

The integral on the right is merely the configuration integral, Z_{1G}, for the ideal gas ($U_N \equiv 0$). Thus, $\langle \exp(+\beta U_N) \rangle$ may be regarded as Z_{1G}/Z. Hence, it is possible to express the excess free energy over the analytically calculable free energy of the ideal gas as

$$\Delta G_{XS} \equiv G_{H_2O} - G_{1G} = -RT \ln(Z/Z_{1G}) = RT \ln \langle \exp(\beta U_N) \rangle \quad (31)$$

Although eq 31 is *formally* correct, severe *practical* computational difficulties render this technique unreliable. This problem has been recognized previously.[19,25] The rest of this section will be a discussion of these difficulties, illustrated by a test calculation that we have performed.

B. Critique of the $\langle \exp(\beta U_N) \rangle$ Technique. The problems can be seen more clearly if the average is expressed in a form different from that in eq 11. If $\exp(\beta U_N)$ is weighted by P_{U_N}, the probability of occurrence of the corresponding value of U_N, then integration over all possible values of U_N gives

$$\langle \exp(\beta U_N) \rangle = \int_{-\infty}^{\infty} P_{U_N}(\nu) \exp(\beta \nu) d\nu \quad (32)$$

The precise determination of ΔG_{XS}, therefore, is equivalent to the precise determination of P_{U_N} around the values of U_N for which the integrand in eq 32 is largest.[25a] In the following paragraphs, we will demonstrate that the range of U_N in which P_{U_N} is computed precisely in a Metropolis MC calculation on liquid water does not include the range of U_N which is important in eq 32. This is a particular manifestation of a general difficulty which hinders the MC calculation of free energy differences between systems which do not resemble each other very closely.[26]

In a MC experiment, P_{U_N} can be determined precisely only for values of U_N which occur with sufficient frequency to be sampled adequately. Generally, P_{U_N} peaks sharply near the mean potential energy. Experimentally,[54] $\langle U_N \rangle \sim -9.9N$ kcal/mol at $T = 298$ K, $P = 1$ atm. The standard deviation ($\sim$ the half-width) of the P_{U_N} distribution is $\sim 1.6\sqrt{N}$ kcal/mol under these conditions, based on the relationship between fluctuations in U_N and the heat capacity.[55] All of the sampling probably will be within a few standard deviations of the mean of P_{U_N} (i.e., $-9.9N$ kcal/mol).

Now let us see which values of U_N must be sampled to evaluate the integral in eq 32 precisely. Since $\beta = 1/RT$ and the logarithm is the inverse of the exponential function, ΔG_{XS} (see eq 31) is a direct measure of the values of U_N which are important for the average of the exponential. Experimentally,[55] for water at $T = 298$ K and $P = 1$ atm, $\Delta G_{XS} = -2.1N$ kcal/mol. In the (T, V, N) ensemble under the same conditions, the excess Helmholtz free energy $\Delta A_{XS} = -5.7N$ kcal/mol.[55] These are much higher than $-9.9N$ kcal/mol, where P_{U_N} is large, because the factor $\exp(\beta U_N)$ vastly increases the importance of high-energy configurations. For example, if $T = 298$ K and $N = 100$, $\exp[\beta(-2.1N)]/\exp[\beta(-9.9N)] \sim 10^{570}$. This explains how high energies can dominate eq 31 and 32 in spite of the extremely low probability of observing the system in such states. We note in passing that this problem does not occur in the calculation of averages such as $\overline{U}_N$, since U_N varies slowly with respect to P_{U_N} so that the integrand $U_N P_{U_N}$ is large where P_{U_N} itself is large (i.e., when $\langle U_N \rangle$ is expressed by analogy to eq 32).

The range of U_N which must be sampled to calculate ΔG_{XS} is $\sim -2.1N - (-9.9N) = 7.8N$ kcal/mol. For $N = 100$, this

corresponds to almost 50 standard deviations of P_{U_N} and is an impossible computational task, using normal Metropolis sampling. In the (T, V, N) ensemble the range is smaller, but this does not improve the feasibility of the calculation.

This same argument can be presented in a different way. In a MC chain with M steps (usually $M \sim 10^6$), events with probability $\ll 1/M$ will not occur, as a practical matter. Above some $U_{N,\mathrm{MAX}}$, for which

$$\int_{U_{N\mathrm{MAX}}}^{\infty} P_{U_N}(\nu)\mathrm{d}\nu \lesssim 1/M$$

the MC calculation will set $P_{U_N} = 0$. Hence, the extreme wings of the P_{U_N} distribution will be undersampled. This has no effect on well-behaved averages such as $\overline{U_N}$, but it is disastrous for $\exp(\beta U_N)$. The calculated excess free energies will be systematically too negative, because of the underweighting of the otherwise dominant high energies.

Figure 2 illustrates P_{U_N} and $P_{U_N}\exp(\beta U_N)$ as obtained for chain II of our water computations. The sharp spike representing $P_{U_N}\exp(\beta U_N)$ occurs at the largest values of U_N actually sampled. As would be predicted by the analysis above, the value $\Delta G_{XS}/N = -8.56$ kcal/mol, calculated from the MC results in Figure 2, is in poor agreement with experiment; 99.9% of the integral in eq 32 comes from the top 0.05% of the energies sampled. The results for chain I are similar, and comparable discrepancies have been obtained in an entirely different liquid system, a model for electrolyte solutions.[56]

Sarkisov et al.[6] report good results, using this technique to calculate the free energy of water in the (T, V, N) ensemble with a pair potential which they have developed. In view of the poor results of our test and the supporting theoretical objections, their agreement with experiment is difficult to understand. The spurious inclusion of a single high energy configuration ($U_N/N \sim -5.7$ kcal/mol) would be sufficient to produce their results, and we must in any case regard them as fortuitous.

Accurate calculations of free energy in liquids are very difficult to obtain, and they are best carried out using specialized sampling techniques.[25,26]

IX. Summary and Conclusions

This paper has demonstrated the feasibility of performing Monte Carlo computations on models for liquid water in the (T, P, N) ensemble. It has been shown that calculations under these conditions make higher demands on the accuracy of the pair potential than do calculations in the (T, V, N) ensemble, since the structure of the fluid seems to be more sensitive to errors in the molar volume than to errors in the pressure caused by inaccuracies in the potential.[57]

Two types of energy probability distribution functions were calculated as probes of the variety of intermolecular interactions in the liquid. The pair interactions between nearest-neighbor molecules are better described as a continuum of bent or stretched hydrogen bonds than as populations of "made" and "broken" hydrogen bonds. The distribution of binding energies indicated that the gradations between the various hydrogen-bonded environments of the molecules also are smooth. Stillinger and Rahman[10] reached similar conclusions by a somewhat different route in their MD study of a water model. Although three-body effects, quantum effects, and coupling to intramolecular degrees of freedom have been neglected (or crudely corrected for), we feel that the agreement of these two independent computer calculations (i.e., MC and MD using two different potential energy functions) is significant evidence for the qualitative relevance of these observations for the real liquid.

Finally, we have demonstrated the inadequacy of a seemingly attractive technique for overcoming the difficult problem of calculating free energies in liquids using the MC method.

Acknowledgment. We would like to thank Dr. L. G. Dunfield for many long and fruitful discussions of Monte Carlo procedures throughout the course of this work.

Appendix. Quantum Effects on the Energy and Heat Capacity

The existence of substantial quantum effects on the thermodynamics of water arises primarily from the small mass of the hydrogen atom and consequent high intra- and intermolecular vibrational frequencies. There are two separate contributions.

First, when a molecule is transferred from the vapor phase to the liquid near room temperature, the sum of the three (unexcited) intramolecular vibrational frequencies decreases by $\sim$435 cm^{-1}.[58] The result is to decrease the intramolecular zero-point energy; $\Delta\mathrm{ZPE}_{\mathrm{INTRA}} = -0.6$ kcal/mol. Since the CI potential was parametrized from ab initio calculations on rigid molecules, it cannot deal with this shift. Hence, $\Delta\mathrm{ZPE}_{\mathrm{INTRA}}$ should be added to the calculated energy for comparison with experiment.[59]

Second, hindered molecular translations and rotations (librations) form two bands of frequencies with IR absorbance maxima near 200 and 700 cm^{-1}, respectively.[60] These values correspond to thermal excitation temperatures of $\sim$300 and $\sim$1000 K, indicating that the vibrations are far from classical at room temperature. This effect is more difficult to treat. We will follow Eisenberg and Kauzmann[61] in viewing the intermolecular vibrations as arising from a collection of quantum-mechanical harmonic oscillators.

The intermolecular vibrational spectral density can be approximated in various ways. Two reasonable ones are (1) two Debye spectra with cutoff frequencies of 200 and 700 cm^{-1}, and (2) two Einstein spectra at average frequencies of 115 and 450 cm^{-1} (as suggested by Falk and Ford[62]). The vibrational thermodynamic properties predicted by the two models are in fairly good agreement. Averaging them, we obtain $E_{\mathrm{V1B}} = 4.4$ kcal/mol (includes 2.7 kcal/mol $\mathrm{ZPE}_{\mathrm{INTER}}$) and $C_{p,\mathrm{V1B}} = 9.6$ cal/mol deg.

The MC results must take account of these quantities before they can be related to the experimental internal energy and heat capacity. This can be done by subtracting the classical vibrational contributions included in the MC results and adding back the full quantum-mechanical vibrational contributions.[63] The classical vibrational *potential* energy for the six intermolecular vibrational modes is $3RT$; $C_{p,\mathrm{POT}}$ contains $3R$ from the same source. Hence, the quantum-corrected equations for the internal energy and the heat capacity, as computed with MC, are

$$\begin{aligned}\overline{E}/N &= \overline{U}_N/N - 3RT + E_{\mathrm{V1B}} + \Delta\mathrm{ZPE}_{\mathrm{INTRA}} \\ &= \overline{U}_N/N + 2.0 \text{ kcal/mol} \qquad (T = 298 \text{ K}) \\ C_p &= C_{p,\mathrm{POT}} - 3R + C_{p,\mathrm{V1B}} \\ &= C_{p,\mathrm{POT}} + 3.6 \text{ cal/mol deg} \qquad (T = 298 \text{ K})\end{aligned}$$

We estimate that the errors in this analysis are ± 0.3 kcal/mol for $\overline{E}/N$ and ± 1 cal/mol deg for C_p, aside from the uncertainties in the MC calculations.

If, instead, the quantum effects were completely ignored and the classical kinetic energy terms were included, one would obtain at $T = 298$ K:

$$\overline{E}/N = \overline{U}_N/N + 1.8 \text{ kcal/mol}$$

$$C_p = C_{p,\mathrm{POT}} + 6.0 \text{ cal/mol deg}$$

The small size of the net quantum correction to $\overline{E}/N$ ($2.0 - 1.8 = +0.2$ kcal/mol) stems from a considerable cancellation of intra- and intermolecular effects. The large $\Delta\mathrm{ZPE}_{\mathrm{INTRA}}$ makes the correction positive even though the intermolecular vibrations are not fully excited.

References and Notes

(1) This work was supported by research grants from the National Science Foundation (PCM75-08691) and from the National Institute of General Medical Sciences of the National Institutes of Health, U.S. Public Health Service (GM-14312).
(2) (a) NIH Trainee. (b) To whom requests for reprints should be addressed.
(3) D. T. Hawkins, *J. Solution Chem.*, **4**, 625 (1975).
(4) J. A. Barker and R. O. Watts, *Chem. Phys. Lett.*, **3**, 144 (1969).
(5) R. O. Watts, *Mol. Phys.*, **28**, 1069 (1974).
(6) G. N. Sarkisov, V. G. Dashevsky, and G. G. Malenkov, *Mol. Phys.*, **27**, 1249 (1974).
(7) G. C. Lie and E. Clementi, *J. Chem. Phys.*, **62**, 2195 (1975).
(8) G. C. Lie, E. Clementi, and M. Yoshimine, *J. Chem. Phys.*, **64**, 2314 (1976).
(9) A. Rahman and F. H. Stillinger, *J. Chem. Phys.*, **55**, 3336 (1971).
(10) F. H. Stillinger and A. Rahman, *J. Chem. Phys.*, **57**, 1281 (1972).
(11) F. H. Stillinger and A. Rahman, *J. Chem. Phys.*, **60**, 1545 (1974).
(12) F. H. Stillinger and A. Rahman, *J. Chem. Phys.*, **61**, 4973 (1974).
(13) A. Rahman, F. H. Stillinger, and H. I. Lemberg, *J. Chem. Phys.*, **63**, 5223 (1975).
(14) J. C. Owicki and H. A. Scheraga, *J. Am. Chem. Soc.*, following paper in this issue.
(15) A. Ben-Naim, "Water and Aqueous Solutions", Plenum, Press, New York, N.Y., 1974.
(16) J. S. Rowlinson, "Liquids and Liquid Mixtures", 2nd ed, Plenum, Press, New York, N.Y., 1969.
(17) T. L. Hill, "An Introduction to Statistical Thermodynamics", Addison-Wesley, Reading, Mass., 1960.
(18) (a) T. M. Apostol, "Mathematical Analysis", Addison-Wesley, Reading, Mass., 1957, p 341; (b) H. Goldstein, "Classical Mechanics", Addison-Wesley, Cambridge, 1950, Chapter 8. For example, in a conventional three-dimensional spherical polar coordinate system with polar angle θ, $J(r, \theta) = r^2 \sin \theta$. It should be noted that, in the simple case where the molecules are point particles (no orientational degrees of freedom) with Cartesian coordinates, $J(\mathbf{X}^N) = 1$.
(19) W. W. Wood in "Physics of Simple Liquids", H. N. V. Temperley, J. S. Rowlinson, and G. S. Rushbrooke, Ed., North-Holland, Publishing Co., Amsterdam, 1968, Chapter 5, p 134.
(20) A. Muenster, "Statistical Thermodynamics", Vol. 1, Springer-Verlag, West Berlin, 1969, p 168 ff.
(21) W. Feller, "An Introduction to Probability Theory and Its Applications", Vol. II, 2nd ed, Wiley, New York, N.Y., 1971, especially Chapter III.
(22) (a) G. Nemethy and H. A. Scheraga, *J. Chem. Phys.*, **36**, 3382 (1962). For subsequent improvements in this theory, see (b) A. T. Hagler, H. A. Scheraga, and G. Nemethy, *J. Phys. Chem.*, **76**, 3229 (1972); (c) B. R. Lentz, A. T. Hagler, and H. A. Scheraga, *ibid.*, **78**, 1531 (1974).
(23) H. C. Andersen, *J. Chem. Phys.*, **61**, 4985 (1974).
(24) L. J. Lowden and D. Chandler, *J. Chem. Phys.*, **61**, 5228 (1974).
(25) Among such quantities are the free energy and entropy, which usually are not expressed as ensemble averages. For more information, see ref 26 or either of the following: (a) G. M. Torrie, "Statistical Mechanics of Small Systems", Thesis, University of Toronto, 1975; (b) G. M. Torrie and J. P. Valleau, *Chem. Phys. Lett.*, **28**, 578 (1974).
(26) J. C. Owicki and H. A. Scheraga, *J. Phys. Chem.*, submitted for publication.
(27) J. M. Hammersley and D. C. Handscomb, "Monte Carlo Methods", Methuen, London, 1964.
(28) N. Metropolis, A. W. Rosenbluth, M. N. Rosenbluth, A. H. Teller, and E. Teller, *J. Chem. Phys.*, **21**, 1087 (1953).
(29) S. Karlin, "A First Course in Stochastic Processes", Academic Press, New York, N.Y., 1969.
(30) This discrete representation is an approximation, but it is exactly the representation of the system used by the computer.
(31) Reference 19, p 147.
(32) J. C. Owicki and H. A. Scheraga, *Chem. Phys. Lett.*, **47**, 600 (1977).
(33) One V step takes $N/2$ times the time for a $\mathbf{X}^N$ step in which the coordinates of only one molecule are changed.
(34) Reference 19, p 153.
(35) For a discussion, see J. C. Owicki, L. L. Shipman, and H. A. Scheraga, *J. Phys. Chem.*, **79**, 1794 (1975).
(36) The EPEN water pair potential developed in this laboratory was applied successfully[35] to potential-energy minimizations on water clusters. However, calculations on liquids involve much larger regions of the pair potential energy hypersurface, and the EPEN potential was found to describe the energies of certain non-hydrogen-bonded repulsive configurations inadequately. An improved version of the potential has been developed (R. A. Nemenoff, J. Snir, and H. A. Scheraga, to be published).
(37) O. Matsuoka, E. Clementi, and M. Yoshimine, *J. Chem. Phys.*, **64**, 1351 (1976). The authors report two parametrizations; E_{INTER} is the one to which we refer.
(38) W. S. Benedict, N. Gailar, and E. K. Plyler, *J. Chem. Phys.*, **24**, 1139 (1956).
(39) A LR potential can be obtained simply by not calculating the exponential functions in the CI potential for large ($R_{OO} \gtrsim 7$ Å) separations, where they are essentially zero. See J. Fromm, E. Clementi, and R. O. Watts, *J. Chem. Phys.*, **62**, 1388 (1975).
(40) I. R. McDonald and K. Singer, *Mol. Phys.*, **23**, 29 (1972).
(41) Any perturbation which would cause $\cos \theta$ to fall outside the range $(-1, 1)$ must be reset to 0 in generating trial configurations. Thus, in those cases, the trial and current values of $\mathbf{X}^N$ have the same value of θ for the perturbed molecule.
(42) W. W. Wood and F. R. Parker, *J. Chem. Phys.*, **27**, 720 (1957).
(43) D. Eisenberg and W. Kauzmann, "The Structure and Properties of Water", Oxford University Press, London, 1969, pp 43–44. The value of C quoted includes a small dipole-induced dipole contribution, which also varies as R^{-6}.
(44) Reference 43, p 190.
(45) N. E. Dorsey, "Properties of Ordinary Water Substance", *ACS Monogr.*, **No. 81** (1940).
(46) G. S. Kell in "Water, a Comprehensive Treatise", Vol. I, F. Franks, Ed., Plenum, Press, New York, N.Y., 1972, Chapter 10.
(47) G. S. Kell, *J. Chem. Eng. Data*, **12**, 66 (1967).
(48) J. C. Owicki, R. A. Nemenoff, J. Snir, and H. A. Scheraga, work in progress.
(49) A. H. Narten and H. A. Levy, *J. Chem. Phys.*, **55**, 2263 (1971).
(50) A. H. Narten, *J. Chem. Phys.*, **56**, 5681 (1972).
(51) The small cusps on the (T, P, N) g_{OO} curves at $R = 4.5$ Å are caused by the discontinuity at the junction between the full CI potential and the LR approximation. This artifact is an insignificant perturbation on the system.
(52) A precise definition of the hydrogen bond is not necessary for our purposes. In general, however, we identify a hydrogen bond with a low interaction energy between two molecules.
(53) (a) Z. W. Salsburg, J. D. Jacobson, W. Fickett, and W. W. Wood, *J. Chem. Phys.*, **30**, 65 (1959); D. A. Chesnut and Z. W. Salsburg, *ibid.*, **38**, 2861 (1963).
(54) $-9.9N$ kcal/mol is the value of $\langle U_N \rangle$ obtained from experiment,[45] neglecting all quantum effects for simplicity.
(55) V. G. Dashevsky and G. N. Sarkisov, *Mol. Phys.*, **27**, 1271 (1974). We have obtained ΔG_{XS} from the value of ΔA_{XS} derived in this reference by considering the effect of the difference in the conditions ($P = 1$ atm vs. $V = 18.07$ cm^3 mol) on the free energy of the ideal gas.
(56) D. N. Card and J. P. Valleau, *J. Chem. Phys.*, **52**, 6232 (1970).
(57) Errors in the pair potential lead to errors in P or V in the (T, V, N) and (T, P, N) ensembles, respectively. If V is free to change, as in the (T, P, N) ensemble, the resultant wrong density (or volume) affects the structure of the liquid much more than does the wrong pressure, when V is fixed at the experimental value in the (T, V, N) ensemble.
(58) Reference 43, p 229. We have taken the mean of the Raman and IR liquid frequencies.
(59) It would be possible to include the coupling of the intra- and intermolecular degrees of freedom in a rigid-body potential either in parametrizing to fit experimental quantities[35] or by preforming ab initio calculations with variable molecular geometry. The latter would be a formidable computational task. The central force model of ref 13 accounts for this effect in a more natural way.
(60) D. A. Draegert, N. W. B. Stone, B. Curnutte, and D. Williams, *J. Opt. Soc. Am.*, **56**, 64 (1966).
(61) Reference 43, p 173. This is a treatment of the intermolecular effects only.
(62) M. Falk and T. A. Ford, *Can. J. Chem.*, **44**, 1699 (1966).
(63) $C_{p,POT}$ (the quantity calculated in a MC experiment) is not identical with the molar configurational heat capacity as discussed by Eisenberg and Kauzmann (ref 43, p 174). These authors considered the total heat capacity to be the sum of contributions from intermolecular vibrations (i.e., hindered translations and rotations) and configurational changes with temperature (i.e., changes in the energetics of the hydrogen-bond network). For example, the configurational C_p of ice is zero (by this definition), but a MC calculation on ice would yield $C_{p,POT} \sim 3R$ from the vibration of the molecules in the lattice. Since LCY did not draw a distinction between $C_{p,POT}$ and the configurational C_p, they overestimated the quantity which should be added to $C_{p,POT}$ ($= C_v'$ in their paper) to compare it with the experimental heat capacity (see later in Appendix). We note that, in most publications on the theory of liquids, $C_{p,POT}$ is called the configurational heat capacity. We have deviated from this practice because the terminology of ref 43 is more common in the literature dealing with liquid water.